



AALBORG UNIVERSITY
DENMARK

Aalborg Universitet

CLIMA 2016 - proceedings of the 12th REHVA World Congress

Heiselberg, Per Kvols

Publication date:
2016

Document Version
Publisher's PDF, also known as Version of record

[Link to publication from Aalborg University](#)

Citation for published version (APA):
Heiselberg, P. K. (Ed.) (2016). CLIMA 2016 - proceedings of the 12th REHVA World Congress: volume 1. Aalborg: Aalborg University, Department of Civil Engineering.

General rights

Copyright and moral rights for the publications made accessible in the public portal are retained by the authors and/or other copyright owners and it is a condition of accessing publications that users recognise and abide by the legal requirements associated with these rights.

- ? Users may download and print one copy of any publication from the public portal for the purpose of private study or research.
- ? You may not further distribute the material or use it for any profit-making activity or commercial gain
- ? You may freely distribute the URL identifying the publication in the public portal ?

Take down policy

If you believe that this document breaches copyright please contact us at vbn@aub.aau.dk providing details, and we will remove access to the work immediately and investigate your claim.

Energy Reduction in Public Building Stock: Assessing the Impact of Control Strategy over Expected Energy Savings and Indoor Comfort Level

Roberto Ruiz Flores^{#1}, Matteo D'Antoni^{*2}, Vincent Lemort^{#3}

*#Energy System Research Unit, Thermodynamics Laboratory
University of Liège, Belgium*

[1r.ruiz@ulg.ac.be](mailto:r.ruiz@ulg.ac.be)

[3vincent.lemort@ulg.ac.be](mailto:vincent.lemort@ulg.ac.be)

**Eurac Research, Institute for Renewable Energy, Bolzano, Italy*

[2matteo.dantoni@eurac.edu](mailto:matteo.dantoni@eurac.edu)

Abstract

In the framework of EU FP7 BRICKER project, the renovation of public owned non-residential buildings is addressed through the installation of innovative passive and active technologies. The expected impact is a primary energy reduction of about 50% with respect to the existing scenario with a large replication potential under different European countries.

In order to achieve such ambitious goal one issue that cannot be ignored is the effect of control strategy, not only over the resulting energy performance but also over the resulting indoor comfort conditions.

In this paper, the actual control strategy implemented in the Belgian demo of Bricker project is introduced, compared against an ideal approach and accordingly optimized. The resulting proposed approach is then tested by means of numerical simulations over a base case scenario before renovation.

The main conclusion of this work is the demonstration that control strategy of energy generation and distribution systems has to be revised whenever deep renovation of passive or active building technologies is undertaken. Contrarily to which, project renovation goals cannot be met.

Keywords: *building renovation, system control strategy, heating system, indoor comfort*

1. Introduction

The present paper focuses on the renovation of a school building demo located in Liège (Belgium). It counts with 22,300 m² of usable area characterized by poor quality of building assemblies, gas-fuel boilers and high-temperature heating terminals. As in similar large buildings, the renovation works will replace existing energy generation systems rather than operate on the existing heating distribution system, mainly because of the large investment costs. Therefore, it is of a very practical interest to understand how regulation of distribution system currently operates in order to guarantee adequate comfort conditions and energy performance before renovation works and also to accomplish with expected energy savings after renovation.

The performance of the heating distribution system and the effectiveness of the control strategy are studied by carrying out detailed numerical simulations.

Through a preliminary energy audit, building characteristics and parameters of the control system were retrieved. A numerical model of heating circuits as well as heating terminals is developed. Both actual control strategy and a proposed one are tested on this model. Indoor air temperature and net energy demand of a monitored zone are used as main performance indicators.

This study demonstrates that existing high-temperature terminals can be effectively exploited even after building’s renovation. Nevertheless, particular care has to be taken in establishing a new regulation of the heating distribution system after renovation in order to avoid discomfort conditions due to indoor overheating. This activity is crucial and a very cost-effective measure also for meeting expected energy savings before renovation.

2. Actual control strategy

Fig. 1. shows the existing heating system which can be ideally divided into primary and secondary loops. The primary loop comprises the energy generation components (gas boilers), whereas the secondary loop consists of the heating distribution and emission devices as well as the circulating pumps and pipes. These loops are separated by an intermediate heat exchanger.

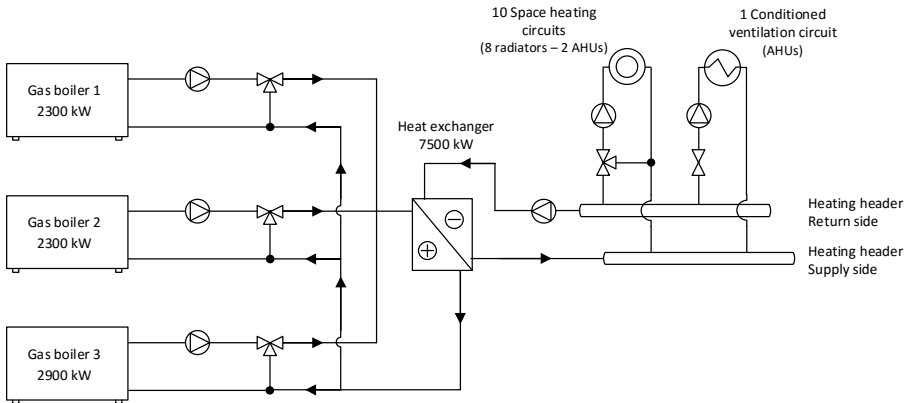


Fig. 1 Existing energy system layout

In total, there are 11 distribution circuits from which: 10 supply hot water for space heating purposes (8 through radiators and 2 through AHUs) and 1 for conditioned ventilation (some small and no centralized AHUs working only few hours in the year).

Regarding to circuits supplying hot water to radiators, they may serve one entire block or a fraction of it depending on the case. This paper focuses on the regulation strategy of the thermal emitted power of radiators connected to this type of circuits.

The radiators’ emitted power is regulated by adjusting uniquely the water supply temperature according to the actual needs of the served block. Since no thermostatic valves are installed, the water flow rate remains constant through them. The regulation is

performed at distribution circuit level by a PI controller configured with a proportional band of 10 K and an integration time of 600 s which acts over the 3-way valve shown in Fig. 1.

The water set point temperature $T_{w,sp}$ to be provided to the controller is calculated from one base temperature and two corrections (1).

$$T_{w,sp} = T_{w,hc} + \Delta T_{wind} + \Delta T_{sol} \quad (1)$$

Where, $T_{w,hc}$ is the base temperature calculated from the system heating curve (2). Looking at the shape, it corresponds to transmission losses at steady state regime. More details about this issue are provided in section 5. ΔT_{wind} is a correction that takes into account infiltration losses (3) and ΔT_{sol} solar gains (4).

$$T_{w,hc} = T_{air,sp} + k \cdot (T_{air,sp} - T_{out})^\alpha \quad (2)$$

$$\Delta T_{wind} = \text{Min}(0.1 \cdot v_{wind}, 5.4) \quad (3)$$

$$\Delta T_{sol} = \text{Max}(-0.01 \cdot I_g, -5) \quad (4)$$

The base temperature $T_{w,hc}$ is calculated in function of the required indoor set point temperature of a specific block ($T_{air,sp}$) and the outdoor dry bulb temperature (T_{out}). The heating curve introduced in (2) is an intrinsic characteristic of the existing control approach which was implemented by the firm Honeywell and cannot be changed. Only modifications to values of coefficient k and exponent α can be performed. Currently, they amount to 4.272 and 0.742 respectively. There is no certainty about the way they were estimated during control implementation phase.

The wind speed correction can range from 0 K to 5.4 K, corresponding to a wind speed of 0 km/h and 54 km/h (or more), respectively. It assumes a linear relationship between wind speed and infiltration losses and also a linear relationship between infiltration losses and temperature correction.

The incident solar radiation correction can range from 0 K to -5 K corresponding to an incident global radiation value of 0 W/m² and 500 W/m² (or more), respectively. It assumes a linear relationship between incident radiation and solar gains and also a linear relationship between solar gains and temperature correction.

Once $T_{w,sp}$ is determined another complementary correction is performed in order to take into account the real state of the indoor temperature T_{air} with respect to the setpoint value $T_{air,sp}$. To do this, only one space of the entire block supplied by a specific distribution circuit is monitored.

The measured deviation between actual and setpoint indoor temperature is used to calculate an equivalent indoor setpoint temperature $T_{air,sp,eqv}$ as shown in (5) which is then introduced in (2) in order to calculate a new ‘‘corrected’’ hot water setpoint temperature.

$$T_{air,sp,eqv} = T_{air,sp} + RF \cdot (T_{air,sp} - T_{air}) \quad (5)$$

From (5), RF is a so-called “room factor”. It corresponds to an empirical value that can vary from 0.1 to 5. A value equal to 1.05 was identified from data provided by Honeywell.

3. Theoretical heating curve

Considering a generic radiator installed into a room and operating at steady state regime. If the over-temperature between radiator and environment (ΔT) is calculated by means of the arithmetic approach [1], the water temperature difference between the inlet and outlet is $\Delta T_w = T_{w,su} - T_{w,ex}$ and the environment temperature is equal to the indoor setpoint ($T_{air,sp}$); then the required water supply temperature to make the radiator covering a certain heating load (\dot{Q}_{rad}) can be calculated as:

$$T_{w,sp} = T_{air,sp} + \left(\frac{\dot{Q}_{rad}}{\dot{Q}_{rad,N}} \right)^{\frac{1}{n}} \cdot \Delta T_N + \frac{1}{2} \cdot \left(\frac{\dot{Q}_{rad}}{\dot{Q}_{rad,N}} \right) \cdot \left(\frac{\dot{m}_{rad,N}}{\dot{m}_{rad}} \right) \cdot \Delta T_{w,N} \quad (6)$$

Where, $\dot{m}_{rad,N}$, $\Delta T_{w,N}$ and $\dot{Q}_{rad,N}$ are the mass flow rate, water temperature difference and the emitted power, respectively, at nominal conditions (test or design). \dot{m}_{rad} is the actual mass flow rate. In the case of this building demo, this value is constant and assumed equal to the nominal one.

The required radiator emitted power (\dot{Q}_{rad}) can be estimated from the enclosed room’s air volume heat balance (assuming steady state) as:

$$\dot{Q}_{rad} = \dot{Q}_{trans} + \dot{Q}_{inf} - \dot{Q}_{sol} - \dot{Q}_{int} \quad (7)$$

In such a way the installed radiator must cover: transmission (\dot{Q}_{trans}) and infiltration losses (\dot{Q}_{inf}). The effect of solar (\dot{Q}_{sol}) and internal (\dot{Q}_{int}) gains (occupants, lighting and appliances) contributes to decrease the heating load required to be covered. A proper definition of the heating curve must consider ideally all these effects.

Comparing the actual approach introduced in section 2 against the one just described, 3 main limitations arise. They are:

- Incomplete number of heat balance components included (3 over 4). Moreover, transmission losses are considered only at steady state regime.
- No proper way to calculate water temperature corrections. The linear superposition of losses and gains of (7) cannot be shifted to water temperature calculation as (1) assumes. Equation (6) shows the effect’s superposition is not linear.
- Not proper way to represent solar gains and infiltration losses: linear relationship between solar gains and incident radiation; and infiltration and wind speed are not correct.

4. Proposed approach

The proposed approach here presented seeks to improve the accuracy in the calculation of the water supply temperature keeping in mind that the structure of heating curve equation and corrections cannot be modified; and the number of required parameters and inputs as well as measured variables cannot be extended. Thus, the proposed approach must maintain the same framework as the original one: one setpoint temperature and one correction according to the actual state of the indoor temperature. Details are provided in the next sections.

A. Water supply temperature

Water supply temperature is calculated by means of (2). Equations (3) and (4) are not used anymore. New parameters k and α are determined from a regression procedure carried out after evaluating (6) by replacing:

$$\dot{Q}_{rad} = \dot{Q}_{UA} = UA \cdot (T_{air,sp} - T_{out}) \quad (8)$$

Where, \dot{Q}_{UA} corresponds to the transmission losses at steady state and UA the heat transfer coefficient by transmission to the external environment of the room or control volume.

Once fitted the parameters, whenever corrections by infiltration losses or radiation gains are required, they are performed by calculating first an equivalent indoor setpoint temperature as:

$$T_{air,sp,eq} = T_{air,sp} + \frac{\dot{Q}_{inf}}{UA} - \frac{\dot{Q}_{sol}}{UA} \quad (9)$$

And then replacing it in (2).

If infiltration losses are considered as:

$$\dot{Q}_{inf} = H_{inf} \cdot (T_{air,sp} - T_{out}) \quad (10)$$

Where, H_{inf} is the heat transfer coefficient by infiltration to the external environment of the room or control volume which corresponds to:

$$H_{inf} = \rho_{air} \cdot \dot{V}_{inf} \cdot C_{p,air} \quad (11)$$

Where in turn, ρ_{air} is the density of dry air equal to 1.204 kg/m^3 , \dot{V}_{inf} the infiltration volumetric flow rate defined as the internal volume of the zone (V_{in}) times the air change rate per hour (ACH) and $C_{p,air}$ the specific heat of dry air equal to $1.012 \text{ kJ/kg} - K$, then k and α can be determined by replacing $\dot{Q}_{rad} = \dot{Q}_{UA} + \dot{Q}_{inf}$ in (6) and the equivalent indoor setpoint temperature to perform water temperature correction due to solar gains is:

$$T_{air,sp,eq} = T_{air,sp} - \frac{\dot{Q}_{sol}}{UA + H_{inf}} \quad (12)$$

In section 5 both options are assessed.

B. Indoor temperature correction

The definition of RF comes from a theoretical analysis. Considering in a specific time a radiator working and emitting power at \dot{Q}_{rad} rate. In that moment the resulting indoor temperature (different to the setpoint) is equal to T_{in} and the energy balance taking place into the room can be defined as in (7). Being \dot{Q}_{heat} the total needed power to cover exactly the heating demand and let the indoor temperature to $T_{air,sp}$, then the required amount of extra power to bring indoor temperature from T_{in} to $T_{air,sp}$ is equal to $\Delta\dot{Q}_{rad} = \dot{Q}_{heat} - \dot{Q}_{rad}$. Assuming also the period to perform this correction is small enough to consider no changes in solar and internal gains. Then $\Delta\dot{Q}_{rad}$ (helped by (7)) corresponds to:

$$\Delta\dot{Q}_{rad} = (\dot{Q}_{trans,h} - \dot{Q}_{trans,r}) + (\dot{Q}_{inf,h} - \dot{Q}_{inf,r}) \quad (13)$$

Subscript “r” corresponds to the actual condition and “h” to the one to accomplish with heating demand.

Finally, considering transmission losses as the sum of two components: one corresponding to steady state losses (\dot{Q}_{UA}) equal to (8) and another corresponding to the energy stored in the walls (\dot{Q}_{stored}) as (14); and infiltration losses as (10).

$$\dot{Q}_{trns} = \dot{Q}_{UA} + \dot{Q}_{stored} \quad (14)$$

Then a corrected indoor setpoint temperature to then be applied in (2) can be defined:

$$T_{air,sp,corr} = T_{air,sp,eq} + CF \cdot (T_{air,sp} - T_{in}) + \frac{\dot{Q}_{stored,h} - \dot{Q}_{stored,r}}{UA} \quad (15)$$

Where:

$$CF = \frac{UA + H_{inf}}{UA} \quad (16)$$

Since no way to evaluate in practice stored energy in walls is possible, the third term of (15) is neglected even risking accuracy in indoor temperature correction. RF is replaced in (5) by a value equal to CF .

If infiltration losses are comprised in the heating curve regression, then $UA + H_{inf}$ should be replaced in (15) and (16) instead of UA . In this case $CF = 1$.

5. Simulation analysis

In the frame of the BRICKER project a detailed energy model of the school building demo was built in TRNSYS environment [2]. The original purpose of this model was to understand the actual energy performance and also to test all the passive and active technologies proposed by the BRICKER project. For this paper, the model is used to test the proposed control approach introduced in section 4.

One circuit is selected (VI) to carry out the simulations and results only for the monitoring zone are analyzed. The main parameters of both thermal zone and installed radiator terminals are provided in Table 1 and Table 2 respectively.

Table 1. Thermal zone characteristics

Parameter	Value	Unit
A_{zone}	446	m ²
V_{in}	2,048	m ³
$A_{wall,ext}$	153	m ²
A_{window}	174	m ²
UA	1.237	kW/K
ACH	0.6	1/h

Table 2. Installed radiator characteristics

Parameter	Value	Unit
$\dot{Q}_{rad,N}$	53.8	kW
n	1.3	-
$\dot{m}_{rad,N}$	3465	kg/h
ΔT_N	48.3	K
$\Delta T_{w,N}$	13.3	K
$T_{w,su,N}$	75	C

Regarding to installed radiator characteristics, since 12 devices are installed in the analyzed zone (in different configurations), values of Table 2 correspond to an equivalent one calculated at design conditions 75/60/20. The mass flow rate at operating conditions is constant and equal to the nominal one ($\dot{m}_{rad} = \dot{m}_{rad,N}$).

Regarding to operation, heating system works during the year within a fixed season which covers the period between weeks 01-19 and 38-52 (15th of September to 15th of May, approximately). For this specific circuit, heating emission system is required to achieve the setpoint value of 20 C only during weekdays from 07:30-16:30. For remaining period and days, a setback temperature of 16 C is defined.

Regarding to simulation parameters, a preconditioning period of one month has been used in order to discard initial simulation periods in which initial conditions might affect simulation results. A simulation time step of 5 minutes is defined.

To assess different alternatives of regulation strategy, 5 yearly simulations are carried. Details about 5 possible scenarios are listed in Table 3.

Table 3. Control parameters for different scenarios

Scenario	k	α	RF
1	4.272	0.742	1.05
2	4.272	0.742	1.05
3	2.766	0.792	1.33
4	3.466	0.793	1.00
5	3.466	0.793	1.00

Scenario 1 corresponds to the actual approach as described in section 2. Scenario 2 uses the same value for parameters k and α but without any correction (solar or infiltration). Scenario 3 corresponds to the proposed approach with k and α obtained only considering transmission losses at steady state without corrections. Scenario 4 comprises transmission and infiltration losses (also proposed approach). Finally, scenario 5 uses the same parameters as 4 but integrates the correction by solar gains in function of incident radiation as shown in Fig. 3. Fig. 2 shows the resulting heating curves for scenarios 3, 4 and 5.

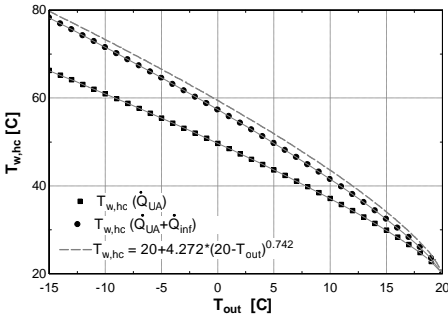


Fig. 2 Ideal v/s fitted heating curve temperature

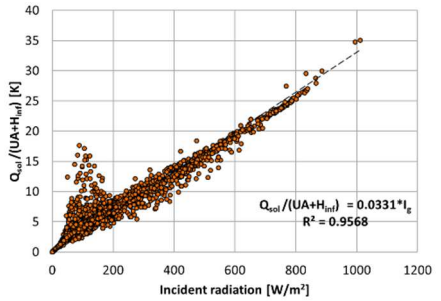


Fig. 3 Solar gain correction

Black squares and circles correspond to the values obtained from (6) as described in section 4A. For both grey lines are the resulting regression curves. Maximum errors in the calculation of water supply temperature of 0.04 K and 0.06 K are induced by both regressions, respectively.

6. Results and discussion

Fig. 4 summarizes by means of a box-and-whisker plot the resulting indoor temperature along the simulation period for those time steps when heating power is required. Values are divided into setpoint hours (left) and setback hours (right).

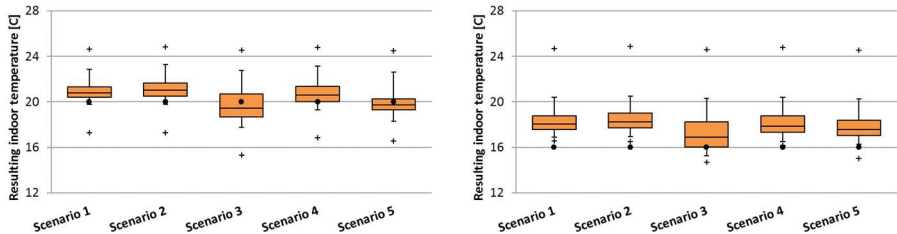


Fig. 4 Box-and-whisker plot of resulting indoor temperature when heating power is needed. Data divided into setpoint hours (left) and setback hours (right).

Upper and lower edges of the orange boxes correspond to the 25th and 75th percentiles. The line at the middle of the box corresponds to the median value of the sample. The whiskers (straight lines) extend to the 5th and 95th percentiles, respectively. Black crosses correspond to minimum and maximum values; and black dots correspond to setpoint and setback temperature values (depending on the graph).

For setpoint hours, the sample's size for 5 scenarios is 1539 hours over 5736 of heating season. Most of the scenarios present high percentage of time above the desired set point value: 91% for scenarios 1 and 2; and 76% for scenario 4. Scenarios 3 and 5 present a 39% and 33% respectively. Scenario 3 is the one that presents the biggest variability with a median value close to the setpoint.

For setback hours, the sample's size for 5 scenarios corresponds to 4021, 3988, 4040, 4003 and 4056 hours respectively. High amount of time considering the lower targeted indoor temperature compared to set point. This fact is caused by the poor quality of the envelope and also the activation system settings. As a common characteristic for all the scenarios is the percentage of time above the defined setback value. The smallest one correspond to scenario 3 with a 76%. All the scenarios overestimate the required water supply temperature for small thermal loads.

In terms of yearly energy demand the results are not that different. In specific terms the values in consecutive order are 181.4, 185.8, 157.9, 178.5 and 167.7 kWh/m²-K.

Taking into account both resulting indoor temperature along the year and heating energy demand, scenario 3 is the optimum among the ones assessed. However, the response is not satisfactory because of the important dispersion around the setpoint value.

Fig. 5 presents the comparison between the water supply temperature obtained by replacing in (6): transmission losses at steady state (\dot{Q}_{UA}) v/s heating demand (\dot{Q}_{heat}) and the difference between heating demand and the stored energy in walls ($\dot{Q}_{heat} - Q_{stored}$) v/s heating demand (\dot{Q}_{heat}). All these heat flows were obtained from another simulation carried out over the model by imposing the indoor temperature (setpoint and setback values) according to the operating schedule introduced in section 5.

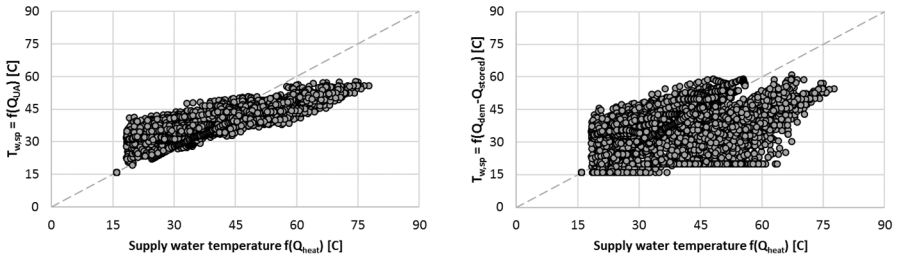


Fig. 5 Supply water temperature in function heating demand versus water temperature from steady state transmission losses (left) and the difference between heating demand and the stored energy in walls.

Fig. 5 (left) shows why scenario 3 resulted to be the best one. The reason is no other than steady state transmission losses profile is the most similar to the resulting heating demand. On the other hand, Fig. 5 (right) compares the resulting water temperature profiles when heating demand is known which means that all the components of the heating balance are known (ideal case) versus the one when all the components are known excepting the stored energy in the opaque envelope. Big dispersion in general between both demonstrates that even being able to predict perfectly all the components of (7) the massive effect of the wall plays key role in the variation of heating demand and cannot be neglected. Big dispersion at lower values (i.e. required water temperature less than 30 C) seems to be the reason of the high over-heating observed during setback hours. To finalize, all this background demonstrates that a better accuracy can be reached if stored energy is included “somehow” in the calculation of indoor temperature correction of (15).

7. Conclusions

In this study, the actual control strategy implemented in the Belgian demo of BRICKER project was presented, compared against an ideal approach, improved and tested by means of numerical simulation.

5 different scenarios were assessed resulting scenario 3 the most optimal in terms of indoor temperature and heating energy demand. All this, given the fixed structure of the control logic in terms equations, parameters to fit as well as the physical variables measured to predict gains and losses of zone’s thermal balance.

The analysis also revealed the importance of the dynamic effects of building envelope in the accuracy of the estimation of water supply temperature. Up to now, it is not included however it should be treated in a future work.

Finally, and for BRICKER project purposes, the main conclusion of this work is the demonstration that control strategy of energy generation and distribution systems has to be revised whenever deep renovation of passive or active building technologies is undertaken. Contrarily to which, project renovation goals cannot be met.

Acknowledgment

The result presented in this paper is part of the BRICKER project (www.bricker-project.com). This project has received funding from the European Union’s Seventh Framework Programme for research, technological development and demonstration under grant agreement No 609071. The information reflects only the author’s view and the Commission is not responsible for any use that may be made of the information it contains.

References

- [1] ASHRAE, 2008. Handbook HVAC systems and equipment. Atlanta: American Society of Heating, Refrigerating and Air-Conditioning Engineers, Inc. 1.
- [2] S.A. Klein, W.A. Beckman, J.W. Mitchell, J.A. Duffie, N.A. Duffie, T.L. Freeman, et al. TRNSYS 17, transient system simulation program. University of Wisconsin, Madison, WI, USA (1979) For more info, <http://sel.me.wisc.edu/TRNSYS>.